https://doi.org/10.1016/j.cej.2023.142216

CO_2-induced reconstruction for ORR-enhanced solid oxide fuel cell cathode

Yuan Zhang[1, 2, ¶], Junbiao Li[1, ¶], Heping Xie[1, *], Zhipeng Liu[1], Suling Shen[1], Ying Teng[1], Daqin Guan[2], Shuo Zhai[1], Yufei Song[3], Wei Zhou[4], Bin Chen[1, 5*], Meng Ni[2, *], Zongping Shao[4, 6]

[1]Guangdong Provincial Key Laboratory of Deep Earth Sciences and Geothermal Energy Exploitation and Utilization, Institute of Deep Earth Sciences and Green Energy, Shenzhen University, Shenzhen 518060, P. R. China

[2]Department of Building and Real Estate, Research Institute for Sustainable Urban Development (RISUD) and Research Institute for Smart Energy (RISE), The Hong Kong Polytechnic University, Hung Hom, Kowloon, Hong Kong, China

[3]Department of Mechanical and Aerospace Engineering, The Hong Kong University of Science and Technology, Clear Water Bay, Hong Kong 999077, China

[4]State Key Laboratory of Materials-Oriented Chemical Engineering, College of Chemical Engineering, Nanjing Tech University, Nanjing 210009, P. R. China

[5]Shenzhen Key Laboratory of Deep Underground Engineering Sciences and Green Energy, Shenzhen 518060, P. R. China

[6]WA School of Mines: Minerals, Energy and Chemical Engineering, Curtin University, Perth, Western Australia 6845, Australia

Corresponding Authors: **Heping Xie** (xiehp@szu.edu.cn); **Bin Chen** (chenbin@szu.edu.cn); **Meng Ni** (meng.ni@polyu.edu.hk)

¶: these authors contributed equally.

Abstract

Solid oxide fuel cell (SOFC) cathode must be highly active and durable for electrochemical

oxygen reduction reaction (ORR). Here, we demonstrate a CO_2-induced reconstruction strategy to build an oxygen incorporative but robust $BaCO_3$ shell for a self-assembled composite cathode from simple $BaFeO_3$ perovskite (noted as re-BF), leading to the enhanced ORR activity, durability, and thermomechanical compatibility. The heterostructure beneath the $BaCO_3$ shell consists of a $BaFeO_3$ phase and a $BaFe_2O_4$ phase, of which $BaFeO_3$ sustains the re-BF with good bulk oxygen transportation. The $BaFe_2O_4$ phase is stable with low thermal expansion coefficient, serving as a reinforced phase to re-BF for better chemical/morphological integrity. This new re-BF cathode shows good durability and a low area-specific resistance (ASR) of 0.013 Ω cm^2, about only one-third of pristine $BaFeO_3$ (0.041 Ωcm^2) at 650°C. This method can also be extended to other perovskite materials to develop an active catalyst for SOFC cathode.

Keywords: Solid oxide fuel cell; Cathode; Reconstruction; Carbon dioxide; Oxygen reduction reaction.

1. Introduction

To date, the solid oxide fuel cell (SOFC) is highly attractive as an energy conversion technology due to its high efficiency, fuel flexibility and low emissions. However, the commercialization of SOFC is not fully successful due to remaining challenges, such as high cost, poor durability and system complexity at the high operating temperature range (700-1000°C)[1]. Lowering the operating temperature and employing cathode materials with both good activity and durability are key solutions to above challenges. An ideal SOFC cathode for low temperature operating should possess high specific area with mixed ion/electron conductivity (MIEC)[2], good chemical/thermomechanical compatibility[3], and more importantly high activity for oxygen reduction reaction (ORR)[4].

Among various cathode candidates, cobalt (Co)-based cathode materials show considerable electrocatalytic activity for the ORR at the intermediate temperature range, such as $Ba_{0.5}Sr_{0.5}Co_{0.8}Fe_{0.2}O_{3-\delta}$ (BSCF) and $La_{0.6}Sr_{0.4}Co_{0.2}Fe_{0.8}O_{3-\delta}$ (LSCF)[5-6]. However, their high thermal expansion coefficient (TEC) limits the durability during thermal cycling. In contrast, cobalt free cathodes, e.g. Fe-based $La_{0.5}Sr_{0.5}FeO_{3-\delta}$ and $BaCe_{0.16}Y_{0.04}Fe_{0.8}O_{3-\delta}$[7–9], have recently attracted particular attention due to their lower TEC and relative higher ORR activity than the Ni and Mn-based counterparts. Besides, much lower price and wider availability of iron can reduce the cost of SOFC[10]. However, most of the Fe-based perovskite oxides represented by $BaFeO_{3-\delta}$ (BF) are unstable in crystal structure. Raw BF powder prepared by the typical sol-gel method is usually a compound with multiple phase structures after the calcination, including triclinic, monoclinic, orthorhombic, cubic and hexagonal perovskite structure[11-12]. Partial substitution with cations become a facile method to stabilize the cubic phase of BF. For example, the reported Bi_2O_3-doped $BaFeO_{3-\delta}$ and La^{3+}-doped $BaFeO_{3-\delta}$ both demonstrate stabilized cubic perovskite-type crystal structure, however their catalytic activity were reduced as a cost[11-13]. To further improve both stability and

activity of BF cathodes, surface and structure optimization at the particle scale are also effective supplementary to the doping method, such as compositing[14-15], surface infiltration[16], atomic layer deposition (ALD)/pulsed laser deposition (PLD) method[17-18], in-situ exsolution[19], electrochemical activation, etc.[20]. It was reported that introducing carbonates on the surface of perovskite can either deactivate or activate the cathodes for ORR depending on the composition method, carbonate species and loading ratio[21-22]. For instance, Hong et al reported that infiltrating proper amount of $BaCO_3$ to BF can facilitate oxygen exchanging kinetics, thus improving the ORR activity[23]. While, if the strontium carbonate was formed through the reaction between perovskite and the CO_2 in air, it will be deactivate the ORR activity since $SrCO_3$ is insulting, pore-blocking and could occupy the original oxygen exchange/transport pathways for cathodes[24]. Therefore, the introduced carbonate demands careful control in terms of the amount, species, and morphology.

Although the morphology control of the additional phases (carbonates or any other functional constitutions) could be versatile, the concept of in-situ reconstruction ("self-assembly" in another word) has been considered as a smart method to introduce new beneficial phases to cathode, since it can provide good adherence, uniform distribution, and rich heterogenous interface. For example, Lu et al. reports a novel simple perovskite nanorod-decorated double perovskite oxide with highly electro-catalytic activity and excellent durability, synthesized by an in-situ exsolving process from a A-site deficient double perovskite host[25]. Even multiphase cathode (≥4 phases) can also be in-situ synthesized to meet the multiple requirements of an ideal cathode[26].

Here, we propose to use in-situ CO_2 treatment to reconstruct the BF, aiming to build a novel composited cathode with its ORR activity and durability significantly enhanced. By the treatment of a certain concentration of CO_2, a novel reconstructed BF cathode (noted as re-BF) is self-assembled with a composite ($BaFe_2O_4$ and $BaFeO_3$) as the core, and a $BaCO_3$

layer as the shell. Such unique morphology and compositions of the new cathode offer two benefits: first, the delicately grown thin shell of carbonate facilitates the surface oxygen incorporation process and charge transfer process, without blocking the pore structure for efficient oxygen diffusion; second, the dual phase core possesses good ORR activity, stable phase structure and low thermal expansion coefficient. As a result, the high-performance cathode re-BF shows greatly enhanced ORR activity with an excellent area-specific resistance (ASR) value of 0.013 Ω cm^2 at 650°C, superior to most cobalt-free cathodes and even comparable with the highly active cobalt-containing perovskites, and can be durably operated for more than 600 hours. This study proposes an innovative strategy to develop high-performance cathodes for low to intermediate temperature SOFCs.

2. Experimental

2.1 Synthesis of powders. The BF powder was synthesized by a combined EDTA-citrate complexing process.[43] The appropriate stoichiometric $Ba(NO_3)_2$, $Fe(NO_3)_3 \cdot 9H_2O$ precursors were all from Sinopharm Chemical Reagent Co., Ltd., analytical grade. The molar ratio of total metal ions: EDTA: citric acid: ammonium ion was 1:1:2:10. The gel was pretreated in a furnace at 250 °C for 24 h to form a solid precursor. The solid precursor was then calcined at 1000 °C for 5 h in air to obtain BF powder. The CO_2-reconstruction BF samples (re-BF) are obtained after BF treated under mixed 10 vol.% CO_2 and 90 vol.% air gas with 100 mL/min [STP] at 650°C for 5 h and then under pure air atmosphere with 100 mL/min [STP] at 650°C for 5 h.

2.2 Fabrication of the symmetrical and single cells. Symmetrical cells with the $Sm_{0.2}Ce_{0.8}O_{1.9}$ (SDC) powder (surface area: 10-14 m^2/g, Fuel-Cell Materials, FCM) as electrolyte were tested and subjected to electrochemical impedance spectroscopy (EIS) measurements. Dense SDC disks of 12 mm diameter and 0.8 mm thickness were prepared by sintering at 1400 °C for 5 h. The cathode ink was made from the glycerol, ethylene glycol,

and isopropyl alcohol mixtures by planetary milling (Fritsch, Pulverisette 6) at 400 rpm for 0.5 h. The suspension was deposited by spray deposition onto both sides of the SDC disk and calcined at 1000 °C for 2 h in air atmosphere to obtain the porous electrodes.

NiO+YSZ/YSZ/SDC anode-supported half-cells were fabricated via a tape-casting process.[3] Then the cathode ink were sprayed over the center of the SDC interlayer surface (with a circular area of 0.45 cm^2) followed by sintering at 1000 °C for 2 h in air. The structure of the finial single cell can be seen in the **Figure S1**. To conduct the infiltration process, infiltration solution was firstly prepared by dissolving barium acetate $Ba(Ac)_2$ (99%, Sinopharm Chemical Reagent Co., Ltd.,) in ethanol. The total metal ion concentrations in this solution was 0.5 mol L^{-1}. The infiltration was carried out by placing a drop of solution on the top of the porous BF backbones, letting the solution soak into the porous backbones, drying, and firing the sample at 650 and 800°C in air 2 h. The sintering temperature of BF backbone is 900°C so that the backbone is highly porous and suitable for infiltration operation.

2.3 Electrochemical testing. The EIS of the symmetrical cells and I-V/I-P curve of single cells were acquired using Princeton PARSTAT 4000+ electrochemical workstations in an in-house fuel cell test station. Regarding the symmetrical test, silver mesh was used as the current collector binding to the cathode surface by silver paste. The cell was placed in CO_2-free air and heated to the target temperature(550-700°C) at 5°C /min to measure the performance of BF electrode. Then, the atmosphere was switched to CO_2 containing air of different concentrations (such as 1%, 5%, and 10% in volume). After 5 hours treatment under open circuit, the electrode is obtained as CO_2-BF. Further, the atmosphere was switched back to CO_2-free air, so that re-BF electrode was formed in-situ. After electrochemical tests of the re-BF, the electrode was naturally cooled down to room temperature in protective CO_2-free air for further characterizations. Regarding the single cell test, the anode side of a button cell was attached to a quartz tube fuel by dry H_2. Glass-ceramic composite is used as the sealant.

At the cathode side, air or CO_2 containing air can be supplied to obtain the CO_2-BF and re-BF. The cell is also heated up to the testing temperature at 5°C /min.

3. Results and discussions

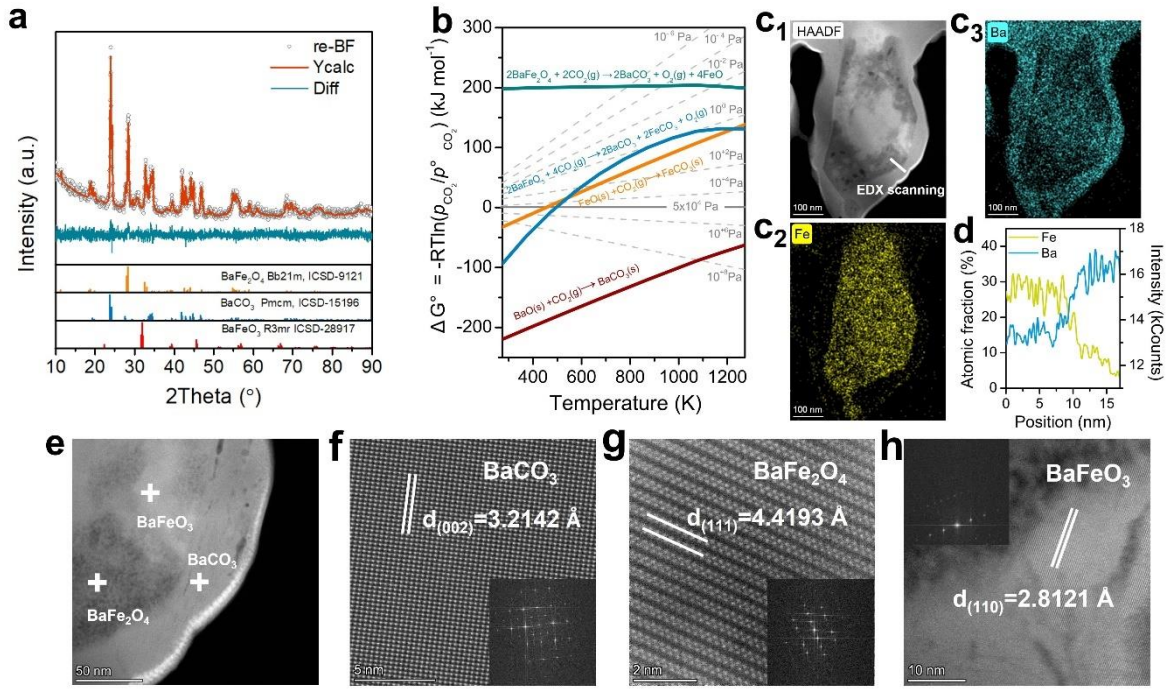

Figure 1. Phase structure and composition of cathodes. a) XRD patterns and XRD refinement results of re-BF, **b)** Ellingham diagram of carbonation of Ba-Fe oxide system, **c)** the STEM-EDX mapping images of re-BF, **d)** line EDX scanning profiles of re-BF, **e-h)** HRTEM images of re-BF.

3.1 Evolution of structure

First, the phase structure of as prepared BF were examined by room-temperature powder X-ray Diffraction (XRD) as shown in **Figure S2a,** which is in good agreement with previous reports[27–29]. We subsequently introduced 10%vol. CO_2 balanced by air to the raw BF at 650°C to form the intermediate noted as CO_2-BF. The XRD result of CO_2-BF was shown in

Figure S2b with additional peaks of carbonates, indicating that the raw BF has patitally converted to barium carbonate. The refinement results of CO_2-BF are in **Figure S3.** Then, we put CO_2-BF back into the air with no CO_2 at 650°C for 5 hours, in order to remove the unstable CO_2 absorbed on the surface, and finally obtain the reconstructed cathode material (re-BF). According to XRD profiles and refinement results for re-BF at room temperature in **Figure 1a and S2c**, the finial re-BF consists of three different phases: the Rhombohedral $BaFeO_3$ phase (space group: R*3mR*, ~6.96 wt.%, a=b=c=4.1231 Å), the Orthorhombic $BaFe_2O_4$ phase (space group: *Bb21m*, ~47.87 wt.%, a=19.0672 Å, b=5.4036 Å and c=8.4711 Å) and a phase of Orthorhombic $BaCO_3$ (space group: *Pmcn*, ~45.17 wt.%, a=5.3159 Å, b=8.9376 Å and c=6.4503 Å)[29]. This refined compostion is also in good agreement with carboantion thermodynamics of various Ba-Fe oxides—as seen from the Ellingham diagram in **Figure 1b,** FeO and $BaFeO_3$ are much less reactive than the BaO to combine with CO_2, incidating that CO_2 thermodynamically prefers to form $BaCO_3$ instead of $FeCO_3$ over the BF surface at the treated temperature and CO_2 partial pressure adopted in this work. Due to the formation of surface-covering $BaCO_3$, of which the Ba source is from the original A site of BF perovskite. Therefore the Ba concentration beneath the surface carbonate shell is reduced, leading to the formation of a $BaFe_2O_4$ phase, that could intimately composite with the remaining $BaFeO_3$ as verified by XRD. Meanwhile, the $BaFe_2O_4$ is thermodynamically more inert than $BaFeO_3$ in carbonization (**Figure 1b**), indicating that the $BaFe_2O_4$ might be a reinfored phase for preventing further carbonization of remaining BF phase. To verify the phase composition and the microtopography of as-reconstruced re-BF, we investigated the microstructures and elemental distribution of re-BF by spherical aberration-corrected transmission electron microscopy (STEM). As shown in **Figure 1c** and **Figure S4**, the morphology of the re-BF was observed to be of a core shell structure. The shell intactly covers the surface of the core of re-BF particles with a thickness of ~25 nm. Based on the

STEM-EDX mapping and line EDX scanning results (**Figure 1d and S4**), the shell mainly contains Ba, C and O elements, while lacks Fe element, confirming the shell is $BaCO_3$. The core compostion is the mixture of $BaFeO_3$ and $BaFe_2O_4$ as verified in **Figure 1e-h** that the three d-spacings of 3.2142, 4.4193 and 2.8121 Å, corresponds to the (002), (111), and (110) planes of $BaCO_3$, $BaFe_2O_4$ and $BaFeO_3$, respectively. In the corresponding fast Fourier transform (FFT) images of **Figure 1e-h**, strong diffraction planes were suggested each phase is well-crystallized, agreeing well with the XRD results.

All the above results suggest a core-shell strucure is fromed after the CO_2 treatment, in which the all three phases are well distributed and intimately connected with the $BaCO_3$ phases as the shell and $BaFe_2O_4$ and $BaFeO_3$ particles as the core. As it is reported that proper amount $BaCO_3$ nanoparticles can enhance ORR kinetics of perovskite cathode [30], suggesting the core shell structure might be a promising high-performance cathode candidate for SOFCs.

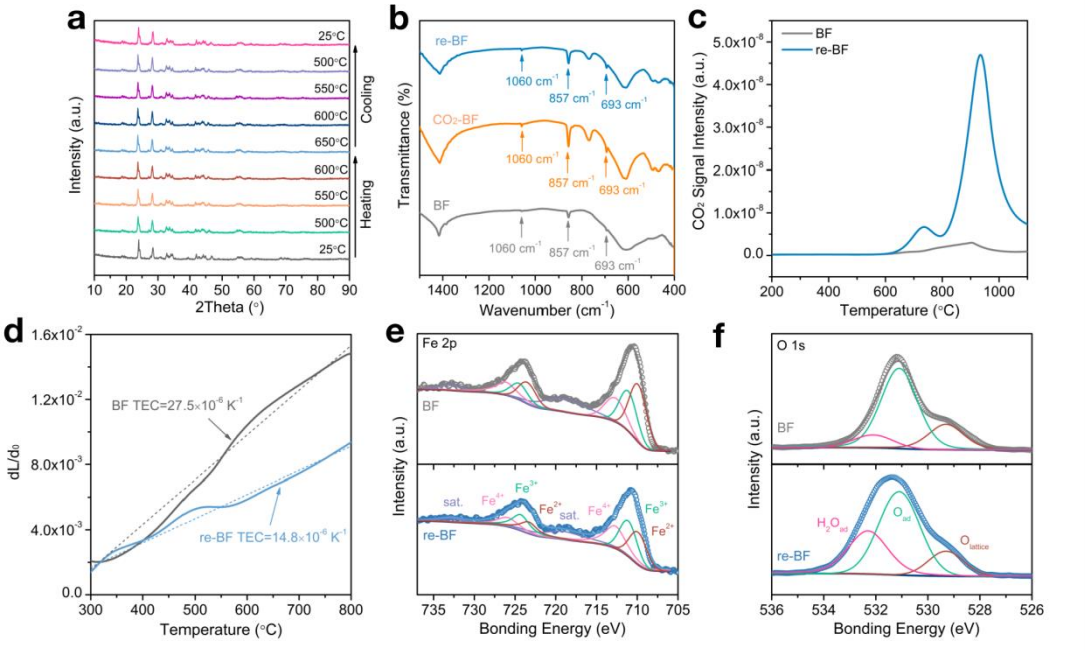

Figure 2. Basic characterization and properties of cathode materials. a) in-situ high temperature XRD profiles for re-BF among 25°C to 650°C, **b)** the FTIR measurement for BF, CO_2-BF, re-BF at room temperature, **c)** the CO_2-TPD curves for BF and re-BF between 200°C to 1100°C, **d)** the TEC measurement for re-BF and BF from 300°C to 800°C, **e)** the

XPS curves of Fe 2p for re-BF and BF and **f)** the XPS curves of O 1s for re-BF and BF.

3.2 Evolution of properties

We also evaluated the phase structural stability of re-BF sample by high-temperature XRD characterization from room temperature to 650°C in air atmosphere (**Figure 2a**). Unlike BF[31], we observed that the phase structure of re-BF did not change significantly as temperature varies. The corresponding refinement results of re-BF at 650°C also reveal that the three phases only slightly changed in amount ($BaFeO_3$ is 9.78%, $BaFe_2O_4$ is 42.15% and $BaCO_3$ is 48.07%) due to the conversion of $BaFe_2O_4$ to $BaFeO_3$, and their lattice parameters are not significantly different from the fresh re-BF at room temperature (**Figure S5**). It suggested the phase structure of re-BF at the investigated temperature range (<650°C) is stable, particularly at the core, otherwise the phase structure change and composition change would lead to large volume change, disintegration, and thus degradation during thermal cycling, i.e. free standing $BaFe_2O_4$[31]. On the other hand, it also indicated the in-situ formed carbonate shell can sustain the air atmosphere as temperature varies, this could also help to comfine the core from disintegration due to phase instabilty of BF and to prevent possible posioning by addtional ditrimental species from air in practical operation.

Fourier transform infrared spectroscopy (FTIR) of cathode materials were also carried out to assess the existence of carbonates. In **Figure 2b**, the peaks of CO_3^{2-} at 693, 857 and 1060 cm^{-1} are evident in both the re-BF and CO_2-BF sample, again proving that the carbonate shell of CO_2-BF is retained in the final re-BF after the air atmosphere treatment. Minor peak of CO_3^{2-} observed for pristine BF should be due to the slight adsorption of CO_2 from air. The shelling of carbonate can be further proved by the CO_2-TPD. As in **Figure 2c**, re-BF exhibits two evident CO_2 desorption peaks at 736°C and 936°C, which is absent in BF, indicating that a small amount of $BaCO_3$ will decompose at ~736°C and a large amount of $BaCO_3$ will

decompose at ~936°C[32]. **Figure S6** showed the TGA test of BF, CO_2-BF and re-BF powders from 300°C to 800°C in air. The results of the TGA test can also prove that the desorption of CO_2 caused the reduction in mass, which is consistent with the results of the CO_2-TPD.

The thermal expansion coefficient (TEC) of pristine BF perovskite and the core shell structured re-BF are also compared. TEC of re-BF is only 14.8×10^{-6} K^{-1} (liner expansion) when heated from 300°C to 800°C (**Figure 2d**), much lower than that of BF (27.5×10^{-6} K^{-1}), which implies better thermal compatibility with electrolyte and long-time durability can be achieved for re-BF than BF[3]. Since the lattice thermal expansion of perovskite is generally attributed to the reduction of transitional metal at B site [33–36], the lower TEC value of re-BF could be due to the less reduction of Fe ions in re-BF (higher fraction of low valance Fe^{2+} in $BaFe_2O_4$ than BF) when the temperature increased. As the TEC of $BaFe_2O_4$ is measured to be 11.6×10^{-6} (Figure S7), which is lower than that of pristine BF. This verifies that the lower Fe valence in $BaFe_2O_4$ can lead to the mitigation of TEC and thus offset the total TEC of re-BF composite. In addition, the shell structure of re-BF could also confine the volume change of particles, which is the second cause for the decrease of TEC[37]. Therefore, this CO_2-induced reconstruction of the cathode materials could effectively reduce the thermal expansion of the electrode and make it match with the electrolyte well.

To further characterize the oxidation states of Fe in both the BF and re-BF, samples were first characterized by X-ray photoelectron spectroscopy (XPS). The fitted plots of Fe 2p profile are deconvoluted into Fe^{2+}, Fe^{3+}, and Fe^{4+} species as shown in **Figure 2e**[36]. The concentrations of Fe^{2+} in re-BF and BF were 41.9% and 30.6%, respectively; For Fe^{3+} in re-BF and BF, the concentrations are 31.0% and 36.4% respectively; For the highest Fe^{4+}, it shows 27.1% in BF and 33.0% in re-BF. It is clear that the average valence of the B-site Fe in BF (~3.024) is higher than that of re-BF (~2.852), which explains the lowered TEC of re-BF

before 800°C since the relatively lower valence of Fe in re-BF are not prone to be further reduced when heated.

From the O 1s XPS result shown, the re-BF possesses a higher concentration of chemically adsorbed oxygen species than that of BF according to the $O_{ad}/O_{lattice}$ ratio (**Figure 2f)**. It therefore verifies that re-BF has more surface oxygen defects that could be beneficial to the oxygen incorporation process and the ORR activity. **Figure 2f** also exhibits that the O 1s binding energies of the lattice oxygen species are 529.3 and 529.7 eV for BF and re-BF, respectively. The higher binding energy implies re-BF are weaker in the Coulombic force between B-site ions and O^{2-}, thus the increased activity of the lattice oxygen[38]. This could be seen as another origin of good ORR activity for the re-BF composite electrode.

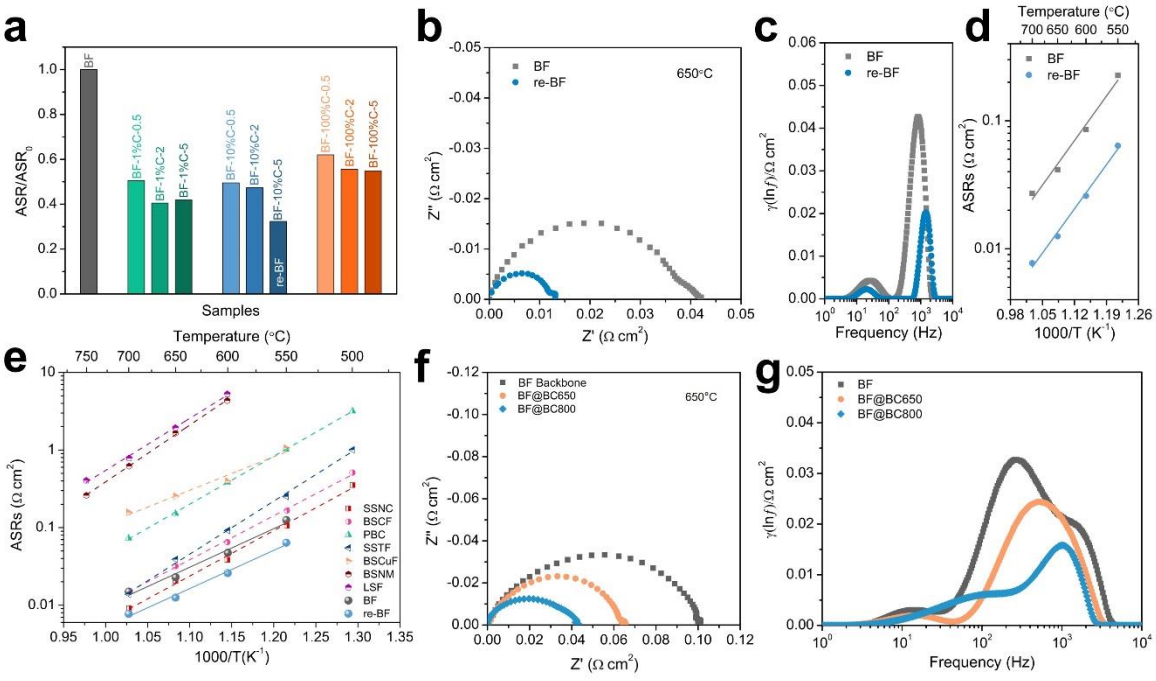

Figure 3. Oxygen reduction reaction performance for symmetrical cells. a) The related change of ASR after 1 vol.%, 10 vol.% and 100 vol.% CO_2 treatment for 0.5 h, 2 h and 5 h at 650°C, the **b)** EIS and **c)** DRT analysis curves for re-BF and BF cathode tested at 650°C, **d)** Arrhenius plots of re-BF and BF cathode, **e)** ASR comparison of BF, re-BF and other

benchmarking cathodes (SSNC: $SrSc_{0.175}Nb_{0.025}Co_{0.8}O_{3-\delta}$, BSCF: $Ba_{0.5}Sr_{0.5}Co_{0.8}Fe_{0.2}O_{3-\delta}$, PBC: $PrBaCo_2O_{5+\delta}$, SSTF: $SrSc_{0.075}Ta_{0.025}Fe_{0.9}O_{3-\delta}$, BSCuF: $Ba_{0.5}Sr_{0.5}Cu_{0.4}Fe_{0.6}O_{3-}$, BSNM: $Bi_2Sr_2Nb_2MnO_{12-\delta}$, LSF: $La_{0.8}Sr_{0.2}FeO_3$.)[39–44], **f)** EIS curves for BF backbone with infiltrated $BaCO_3$ fired at 650°C (BF@BC650) and 800°C (BF@BC800) *v.s.* BF backbone tested at 650°C, **g)** DRT analysis for BF cathode with infiltrated $BaCO_3$.

3.3 Electrochemical evaluation of the re-BF composite

The oxygen reduction reaction performances of above materials were firstly quantified using electrochemical impedance spectroscopy (EIS) in $Sm_{0.2}Ce_{0.8}O_{1.9}$(SDC) based symmetrical cells. The ASR values of a re-BF|SDC|re-BF symmetrical cell were tested between 550 °C and 700 °C in air. For comparison, we also measured the ASRs (650°C, in air) of pristine BF and the BF cathode after the treatment of CO_2 at different concentrations (1%, 10% and 100%) for different time (0.5 h, 2 h and 5 h) that are termed as BF-CO_2%-time (**Figure S8**). In **Figure 3a**, we defined the ratio of measured ASR after CO_2 treatment to the original ASR before CO_2 treatment as ASR/ASR_0 index for better comparison. It can be seen that the ASR/ASR_0 of all the samples are greatly reduced after reconstruction by CO_2, the most ORR-enhanced sample (10% CO_2 treated for 5 h) is termed as the re-BF sample, showing only 0.013 Ω cm^2, about one third of BF (0.041 Ω cm^2) at 650°C as compared in **Figure 3b** (without ohmic resistance) and **Figure S9** (with ohmic resistance), indicating a very significant ORR activity enhancement in the re-BF cathode.

To gain insights into the enhancement mechanism, we investigated the key rate-determining steps for the ORR process in both BF and re-BF by employing the distribution of relaxation time (DRT) technique to interpret the EIS results[4,44]. **Figure 3c** displays the DRT curves for BF and re-BF symmetrical cells at 650°C. Each curve reveals two major peaks—a high frequency peak (HF, 10^2~10^4 Hz) and a low frequency peak (LF, 10^0~10^2 Hz), which

can be ascribed to charge transfer/oxygen incorporation and diffusion processes, respectively[14]. Notably, both the HF and LF peaks of re-BF decrease, indicating that charge transfer and surface oxygen incorporation processes are improved by CO_2 reconstruction, which could be possible due to blocking effect of carbonate in carbonate-perovskite composite[15]. The oxygen gas diffusion process is not hindered due to the unblocked pore structure as seen in Figure S10a.

Figure 3d compares the Arrhenius plots of ASRs for BF and re-BF cathodes from 550 to 700°C. Apparently, re-BF exhibits better ASRs at values of 0.008, 0.013, 0.026, and 0.064 $\Omega\,cm^2$ at 700, 650, 600, and 550 °C, respectively, that are much enhanced at variant temperatures than BF cathode, of which ASRs values are 0.027, 0.041, 0.086, and 0.227 $\Omega\,cm^2$ at 700, 650, 600, and 550 °C, respectively. Accordingly, the cathodic activation energy E_a of the BF and re-BF are 95.20 kJ mol^{-1} and 94.49 kJ mol^{-1}. **Figure 3e** displays the enhanced re-BF electrode demonstrates almost the best ORR activity compared to benchmarking cathodes such as cobalt-free $La_{0.8}Sr_{0.2}FeO_3$(LSF), $Sc_{0.075}Ta_{0.025}Fe_{0.9}O_{3-\delta}$(SSTF), $Ba_{0.5}Sr_{0.5}Cu_{0.4}Fe_{0.6}O_{3-\delta}$(BSCuF) and $Bi_2Sr_2Nb_2MnO_{12-\delta}$(BSNM), even higher than state-of-art cobalt cathodes, such like $Ba_{0.5}Sr_{0.5}Co_{0.8}Fe_{0.2}O_{3-\delta}$(BSCF), $SrSc_{0.175}Nb_{0.025}Co_{0.8}O_{3-\delta}$(SSNC) and $PrBaCo_2O_{5+\delta}$(PBC) [39–44].

Considering the complicated composition of re-BF, it is still needed to distinguish which phase or phases are playing the key role in enhancing the ORR activity. Therefore, we design a modified BF cathode by infiltrating 10wt% barium acetate directly to the BF cathode and then calcinating to generate $BaCO_3$[23]. **Figure 3f and g** showcase the variation of EIS and DRT curves for modified BF cathodes after $BaCO_3$ infiltration that was calcinated at 650°C(BF@BC650) and 800°C(BF@BC800). As seen, the existence of carbonate reduces the polarization resistance, confirming the positive effect of $BaCO_3$ on ORR activity. The BF@BC800 is more ORR active, possibly due to the infiltrated barium acetate cannot be

fully converted to $BaCO_3$ completely at 650°C. More importantly, we can find that HF peaks for BF@BC800 were decreased after the infiltration, which means the charge transfer and oxygen incorporation process were facilitated. In contrast, the LF peaks were increased, probably because the direct composition with barium carbonate through infiltration could block the pore structure thus impeding the oxygen gas diffusion, as seen from Figure S10b that pores are filled by carbonates. This suggests that Ba carbonate compositing can be effective for optimizing the ORR only when ingenious morphology and amount control of carbonate are premised. The CO_2 re-construction used in this work for preparing the thin filmed re-BF in an intimate carbonate shell can be a mild but smart method to avoid the countereffects from carbonate.

Besides, we also need to elucidate whether the $BaFe_2O_4$ in the core phase of re-BF cathode is beneficial to the ORR catalytic activity. The ASR of $BaFe_2O_4$ was measured (**Figure S11)** to be much worse than that of the original BF, but the ASR is greatly reduced after adding a small amount (20 wt.%) of $BaFeO_3$, indicating that although the outstanding ORR activity of re-BF is not originated from the nonconductive $BaFe_2O_4$, the generation of $BaFe_2O_4$ will not largely influence unless the amount of inert $BaFe_2O_4$ is excessive. In additional, it is also likely the rich hetero-interfaces between $BaFeO_3$ and $BaFe_2O_4$ generated during the re-assembly process can serves as a fast routine for oxygen ion transportation through surface oxygen diffusion as reported[27].

In terms of the cathode durability, the carbonate shell and in-core $BaFe_2O_4$ are both less thermal expansive than $BaFeO_3$ and both more stable in phase structure at the operating temperature of SOFC. In addition, $BaFe_2O_4$ is more less reactive with CO_2 atmosphere (**Figure 1b**) and supports the structural stability of re-BF bulk phase from excessive carbonization if operated in practical SOFC operation with trace CO_2 in air.

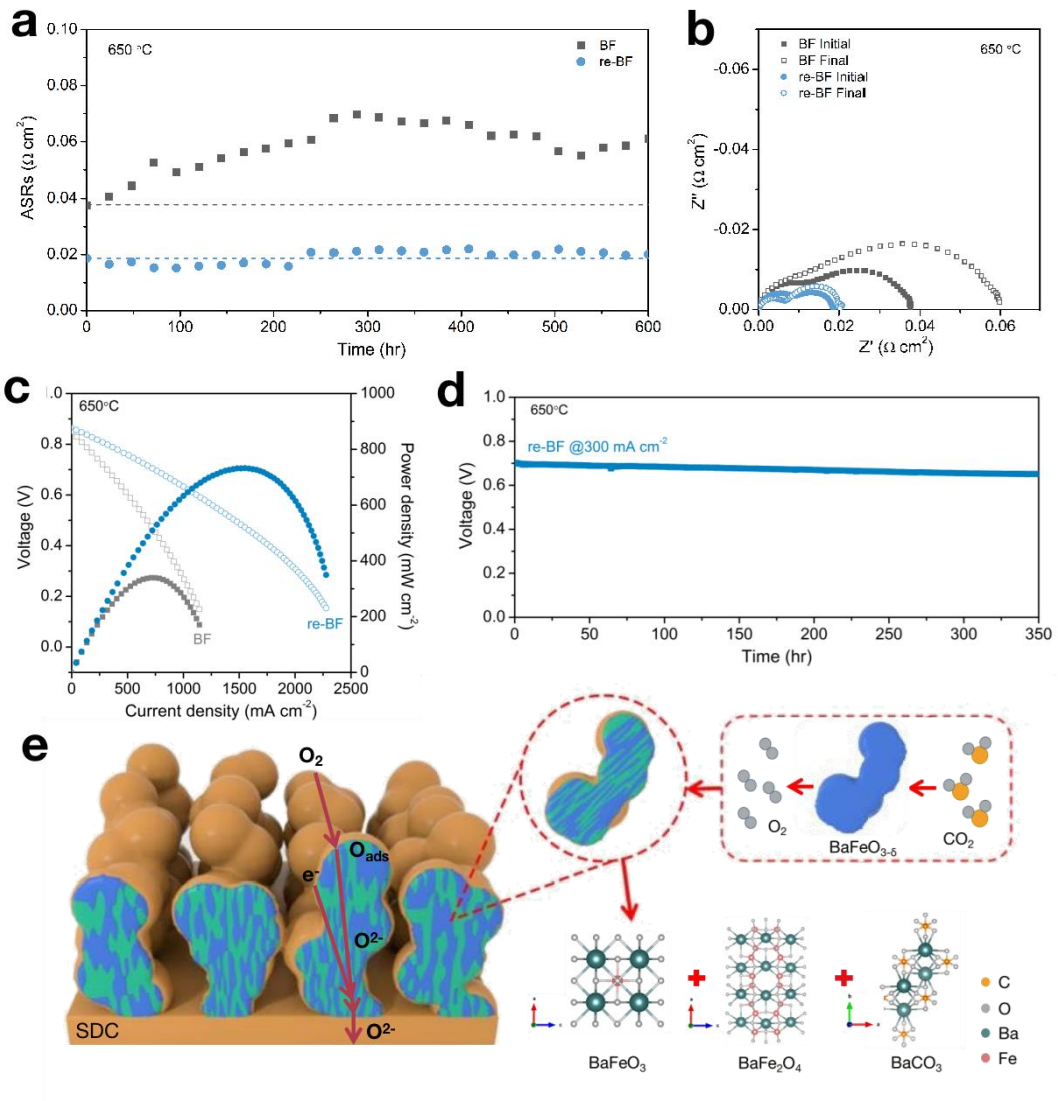

Figure 4. Cathode durability, single cell performance and schematic diagram of electrode. a) 600 hours durability of the ASR values of BF and re-BF cathode at 650°C, **b)** EIS curves of BF and re-BF cathode before and after the durability test, **c)** I-V curves of re-BF and BF cathode in Ni/YSZ|YSZ|SDC anode supported single cell, **d)** re-BF single cell durability at 650°C for 350 hours, **e)** schematic process of CO_2-induced reconstruction in re-BF cathode.

3.4 Performance and durability of re-BF cathode

Figure 4a shows the long-time durability of BF and re-BF cathodes of symmetrical cells during 600 hours at 650°C in air. From 0 to 600 hours, the ASR of the re-BF cathode

increased only from 0.0187 to 0.0201 Ω cm^2, and the degradation rate is as slow as 0.0023 Ω cm^2 per 1000 h. It demonstrates the superior durability of the re-BF electrode. **Figure 4b** shows the EIS change of BF and re-BF after the long-term stability test. It can be seen that the impedance of BF increases significantly (from 0.0376 to 0.0598 Ω cm^2, 0.037 Ω cm^2 per 1000 h), while re-BF remains almost unchanged. As for the stability of crystal structure, the XRD patterns of re-BF and BF cathode powder after a 600 h treatment in air at 650°C shows there is no phase change for re-BF (**Figure S12**), while the BF sample contains additional peaks, that can be attributed to be Ba segregation. The above durability test showcases the effectiveness of carbonates shell in improving the durability of re-BF as the cathode.

Finally, the cathode performance is also evaluated on a full single cell, fabricated with a NiO+YSZ/YSZ/SDC/cathode structure. The re-BF cathode exhibits a superior performance enhancement ratio, achieving 2.1 times increased peak power density when compared to the counterpart cell with BF as the cathode (735 mW cm^{-2} *v.s.* 350 mW cm^{-2} at 650°C in **Figure 4c**). A 350-hour durability test at 300 mA cm^{-2}, 650°C (**Figure 4d**) shows the re-BF cathode is of an excellent durability in practical full cell operation. **Figure 4f** shows the schematic process of CO_2-induced reconstruction in re-BF cathode. All the above results suggest a core-shell strucure is fromed by the CO_2 treatment, in which the $BaFe_2O_4$, $BaFeO_3$ and $BaCO_3$ phases are well distributed and intimately connected, with the $BaCO_3$ phases as shell and $BaFe_2O_4$ and $BaFeO_3$ particles as core. It is well known that $BaCO_3$ nanoparticles can enhance ORR kinetics of the charge transfer process and the core can improve the stability, the core shell structure gives a potential high-performance cathode candidate for SOFCs with improved ORR kinetics.

4. Conclusions

In summary, we developed the CO_2-induced reconstruction method for enhancing the ORR activity and durability of SOFC cathode. This method employed the high temperature CO_2 treatment to reconstruct pristine BF perovskite to form a new re-BF composite cathode with a core-shell structure—an external $BaCO_3$ shell and a dual phase core ($BaFe_2O_4$ phase and $BaFeO_3$ phase) which synergistically benefit the charge transfer, surface oxygen incorporation, and the durability. As a result, the re-BF cathode yields a recording-high ORR activity ($0.013\ \Omega\,cm^2$ at 650ºC), and demonstrates good durability for over 600 h. The re-BF single cell exhibits a superior performance with 735 mW cm^{-2} peak power density at 650°C. This work opens up new possibilities for cathode optimization by facile reconstruction for solid oxide fuel cells.

5. CRediT authorship contribution statement

Yuan Zhang: Designed project, Performed experiments, Analyzed data, Wrote original draft and Revised. **Junbiao Li:** Performed characterizations and experiments, Analyzed data. **Heping Xie:** Designed project, Contributed laboratory, Supervision. **Zhipeng Liu:** Helped experiments. **Daqin Guan:** Analyzed XRD data. **Shuo Zhai:** Provide analysis tools. **Yufei Song, Suling Shen, Ying Teng:** Helped to analyse data, Revised draft. **Wei Zhou:** Provide analysis tools. **Bin Chen:** Designed project, Wrote original draft and Revised. **Meng Ni:** Designed project, Contributed laboratory, Revised draft. **Zongping Shao:** Designed project, Revised draft. All authors reviewed the manuscript.

6. Declaration of Competing Interest

The authors declare that they have no known competing financial interests or personal relationships that could have appeared to influence the work reported in this paper.

7. Acknowledgements

This work was supported by National Natural Sciences Foundation of China (No. 52006150, No. 22109101, No. 62205212), Program for Guang-dong Introducing Innovative and Entrepreneurial Teams (Grant No. 2019ZT08G315), Shenzhen Science and Technology Program (Grant No. RCBS20210609103648039 and No. JCYJ20210324093008021), the fellowship of China postdoctoral science foundation (No. 2021T140471). M. Ni gratefully acknowledge the support provided by the Project of Strategic Importance funding scheme (Project ID: P0035168) from The Hong Kong Polytechnic University.

8. Data availability

The data that support the findings of this study are available from the corresponding author upon reasonable request.

9. Supplementary material

Supplementary data associated with this article can be found in the online version.

10. References

[1] Shao, Z. & Hale, S. M. A high-performance cathode for the next generation of solid-oxide fuel cells. Nature 431, 170–174 (2004).

[2] Zhang, Y. *et al.* Recent progress on advanced materials for solid-oxide fuel cells operating below 500 °C. *Adv. Mater.* **29**, 1700132 (2017).

[3] Zhang, Y. *et al.* Thermal-expansion offset for high-performance fuel cell cathodes. *Nature* **591**, 246–251 (2021).

[4] Kotomin, E. A., Mastrikov, Y. A., Merkle, R. & Maier, J. First principles calculations of oxygen reduction reaction at fuel cell cathodes. *Curr. Opin. Electrochem.* **19**, 122–128 (2020).

[5] Lin, Y. *et al.* Evaluation of $Ba_{0.5}Sr_{0.5}Co_{0.8}Fe_{0.2}O_{3-\delta}$ as a potential cathode for an anode-supported proton-conducting solid-oxide fuel cell. *J. Power Sources* **180**, 15–22 (2008).

[6] Fabbri, E., Bi, L., Pergolesi, D. & Traversa, E. High-performance composite cathodes with tailored mixed conductivity for intermediate temperature solid oxide fuel cells using proton conducting electrolytes. *Energy Environ. Sci.* **4**, 4984–4993 (2011).

[7] Simner, S. P. *et al.* Development of lanthanum ferrite SOFC cathodes. *J. Power Sources* **113**, 1–10 (2003).

[8] Zou, D. *et al.* The $BaCe_{0.16}Y_{0.04}Fe_{0.8}O_{3-\delta}$ nanocomposite: a new high-performance cobalt-free triple-conducting cathode for protonic ceramic fuel cells operating at reduced temperatures. *J. Mater. Chem. A* **10**, 5381–5390 (2022).

[9] Dailly, J. & Fourcade, S. a. Largeteau, F. Mauvy, JC Grenier and M. Marrony. *Electrochim. Acta* **55**, 5847–5853 (2010).

[10] Lu, Y. *et al.* Investigation of In-doped $BaFeO_{3-\delta}$ perovskite-type oxygen permeable membranes. *J. Mater. Chem. A* **3**, 6202–6214 (2015).

[11] Song, X. *et al.* High performance $BaFe_{1-x}Bi_xO_{3-\delta}$ as cobalt-free cathodes for intermediate temperature solid oxide fuel cells. *Int. J. Hydrogen Energy* **42**, 15808–15817 (2017).

[12] Kida, T. *et al.* Oxygen permeation properties of partially A-site substituted $BaFeO_{3-\delta}$ perovskites. *J. Electrochem. Soc.* **156**, E187 (2009).

[13] Dong, F., Chen, D., Chen, Y., Zhao, Q. & Shao, Z. La-doped $BaFeO_{3-\delta}$ perovskite as a cobalt-free oxygen reduction electrode for solid oxide fuel cells with oxygen-ion conducting electrolyte. *J. Mater. Chem.* **22**, 15071 (2012).

[14] Abd Aziz, A. J., Baharuddin, N. A., Somalu, M. R. & Muchtar, A. Review of composite cathodes for intermediate-temperature solid oxide fuel cell applications.

Ceram. Int. **46**, 23314–23325 (2020).

[15] Juhl, M., Primdahl, S., Manon, C. & Mogensen, M. Performance/structure correlation for composite SOFC cathodes. *J. Power Sources* **61**, 173–181 (1996).

[16] Ding, D., Liu, M. & Liu, M. Enhancing sofc electrode performance through surface modification. *ECS Trans.* **57**, 1801–1810 (2013).

[17] Yu, A. S., Küngas, R., Vohs, J. M. & Gorte, R. J. Modification of sofc cathodes by atomic layer deposition. *J. Electrochem. Soc.* **160**, F1225–F1231 (2013).

[18] Choi, H. J. *et al.* Surface tuning of solid oxide fuel cell cathode by atomic layer deposition. *Adv. Energy Mater.* **8**, 1802506 (2018).

[19] Sun, Y.-F. *et al.* New opportunity for in situ exsolution of metallic nanoparticles on perovskite parent. *Nano Lett.* **16**, 5303–5309 (2016).

[20] Zhang, X. *et al.* Enhanced electrochemical property of $La_{0.6}Sr_{0.4}Co_{0.8}Fe_{0.2}O_3$ as cathode for solid oxide fuel cell by efficient in situ polarization-exsolution treatment. *Electrochim. Acta* **258**, 1096–1105 (2017).

[21] Mutoro, E., Crumlin, E. J., Biegalski, M. D., Christen, H. M. & Shao-Horn, Y. Enhanced oxygen reduction activity on surface-decorated perovskite thin films for solid oxide fuel cells. *Energy Environ. Sci.* **4**, 3689 (2011).

[22] Zhu, Y., Sunarso, J., Zhou, W. & Shao, Z. Probing CO_2 reaction mechanisms and effects on the $SrNb_{0.1}Co_{0.9-x}Fe_xO_{3-\delta}$ cathodes for solid oxide fuel cells. *Appl. Catal. B Environ.* **172**–**173**, 52–57 (2015).

[23] Hong, T., Brinkman, K. S. & Xia, C. Barium carbonate nanoparticles as synergistic catalysts for the oxygen reduction reaction on La0. 6Sr0. $4Co_{0.2}Fe_{0.8}O_{3-\delta}$ solid-oxide fuel cell cathodes. *ChemElectroChem* **3**, 805–813 (2016).

[24] Fidelsky Kozokaro, V. & Caspary Toroker, M. Perovskite $La_{0.3}Sr_{0.7}Fe_{0.7}Cr_{0.3}O_{3-\delta}$ catalysis raises the bar: preventing unwanted near-surface sr segregation and $SrCO_3$

precipitation. *Adv. Theory Simulations* **5**, 2100173 (2022).

[25] Lu, F. *et al.* Heterostructured simple perovskite nanorod-decorated double perovskite cathode for solid oxide fuel cells: Highly catalytic activity, stability and CO_2-durability for oxygen reduction reaction. *Appl. Catal. B Environ.* **249**, 19–31 (2019).

[26] Song, Y. *et al.* A cobalt-free multi-phase nanocomposite as near-ideal cathode of intermediate-temperature solid oxide fuel cells developed by smart self-assembly. *Adv. Mater.* **32**, 1906979 (2020).

[27] He, W. *et al.* Zr doped $BaFeO_{3-\delta}$ as a robust electrode for symmetrical solid oxide fuel cells. *Int. J. Hydrogen Energy* **44**, 32164–32169 (2019).

[28] Dong, F., Chen, Y., Chen, D. & Shao, Z. Surprisingly high activity for oxygen reduction reaction of selected oxides lacking long oxygen-ion diffusion paths at intermediate temperatures: a case study of cobalt-free $BaFeO_{3-\delta}$. *ACS Appl. Mater. Interfaces* **6**, 11180–11189 (2014).

[29] Niu, Y. *et al.* A single-step synthesized cobalt-free barium ferrites-based composite cathode for intermediate temperature solid oxide fuel cells. *Electrochem. commun.* **13**, 1340–1343 (2011).

[30] Hong, T., Chen, F. & Xia, C. Barium carbonate nanoparticle as high temperature oxygen reduction catalyst for solid oxide fuel cell. *Electrochem. Commun.* **51**, 93–97 (2015).

[31] Hong, T., Chen, F. & Xia, C. Barium carbonate nanoparticle to enhance oxygen reduction activity of strontium doped lanthanum ferrite for solid oxide fuel cell. *J. Power Sources* **278**, 741–750 (2015).

[32] Nichols, M. & Lafferty Jr, R. Decomposition temperatures of some analytical precipitates. barium carbonate. *Ind. Eng. Chem. Anal. Ed.* **14**, 481–485 (1942).

[33] Ramaswamy, V., Awati, P. & Tyagi, A. K. Lattice thermal expansion of

$LaCo_{1-x}Cu_xO_3$. *J. Alloys Compd.* **364**, 180–185 (2004).

[34] Zhu, Q., Jin, T. & Wang, Y. Thermal expansion behavior and chemical compatibility of $Ba_xSr_{1-x}Co_{1-y}Fe_yO_{3-\delta}$ with 8YSZ and 20GDC. *Solid State Ionics* **177**, 1199–1204 (2006).

[35] Jiang, S. *et al.* Cobalt-free $SrNb_xFe_{1-x}O_{3-\delta}$ (x= 0.05, 0.1 and 0.2) perovskite cathodes for intermediate temperature solid oxide fuel cells. *J. Power Sources* **298**, 209–216 (2015).

[36] Zhou, W., Jin, W., Zhu, Z. & Shao, Z. Structural, electrical and electrochemical characterizations of $SrNb_{0.1}Co_{0.9}O_{3-\delta}$ as a cathode of solid oxide fuel cells operating below 600°C. *Int. J. Hydrogen Energy* **35**, 1356–1366 (2010).

[37] Nie, S., Liu, Y., Liu, Q., Wang, M. & Wang, H. Phase transitions and thermal expansion of $BaCO_3$ and $SrCO_3$ up to 1413 K. *Eur. J. Mineral.* **29**, 433–443 (2017).

[38] Zhang, Z., Zhu, Y., Zhong, Y., Zhou, W. & Shao, Z. Anion doping: a new strategy for developing high-performance perovskite-type cathode materials of solid oxide fuel cells. *Adv. Energy Mater.* **7**, 1700242 (2017).

[39] Zhang, Y. *et al.* Significantly improving the durability of single-chamber solid oxide fuel cells: a highly active CO_2-resistant perovskite cathode. *ACS Appl. Energy Mater.* **1**, 1337–1343 (2018).

[40] Song, K. W. & Lee, K. T. Characterization of $Ba_{0.5}Sr_{0.5}M_{1-x}Fe_xO_{3-\delta}$ (M = Co and Cu) perovskite oxide cathode materials for intermediate temperature solid oxide fuel cells. *Ceram. Int.* **38**, 5123–5131 (2012).

[41] Zhu, Y., Zhou, W., Chen, Y. & Shao, Z. An aurivillius oxide based cathode with excellent CO_2 tolerance for intermediate-temperature solid oxide fuel cells. *Angew. Chemie* **128**, 9134–9139 (2016).

[42] Yan, A., Maragou, V., Arico, A., Cheng, M. & Tsiakaras, P. Investigation of a

$Ba_{0.5}Sr_{0.5}Co_{0.8}Fe_{0.2}O_{3-\delta}$ based cathode SOFC. II. The effect of CO_2 on the chemical stability. *Appl. Catal. B Environ.* **76**, 320–327 (2007).

[43] Zhang, Y. *et al.* Evaluation of the CO_2 poisoning effect on a highly active cathode $SrSc_{0.175}Nb_{0.025}Co_{0.8}O_{3-\delta}$ in the oxygen reduction reaction. *ACS Appl. Mater. Interfaces* **8**, 3003–3011 (2016).

[44] Zhang, Y. *et al.* Enhanced oxygen reduction kinetics of IT-SOFC cathode with $PrBaCo_2O_{5+\delta}/Gd_{0.1}Ce_{1.9}O_{2-\delta}$ coherent interface. *J. Mater. Chem. A* **10**, 3495–3505 (2022).

Supporting Information

CO_2-induced reconstruction for ORR-enhanced perovskite cathode

Yuan Zhang[1, 2, ¶], Junbiao Li[1, ¶], Heping Xie[1, *], Zhipeng Liu[1], Suling Shen[1], Ying Teng[1], Daqin Guan[2], Shuo Zhai[1], Yufei Song[3], Wei Zhou[4], Bin Chen[1, 5*], Meng Ni[2, *], Zongping Shao[4, 6]

[1]Guangdong Provincial Key Laboratory of Deep Earth Sciences and Geothermal Energy Exploitation and Utilization, Institute of Deep Earth Sciences and Green Energy, Shenzhen University, Shenzhen 518060, P. R. China

[2]Department of Building and Real Estate, Research Institute for Sustainable Urban Development (RISUD) and Research Institute for Smart Energy (RISE), The Hong Kong Polytechnic University, Hung Hom, Kowloon, Hong Kong, China

[3]Department of Mechanical and Aerospace Engineering, The Hong Kong University of Science and Technology, Clear Water Bay, Hong Kong 999077, China

[4]State Key Laboratory of Materials-Oriented Chemical Engineering, College of Chemical Engineering, Nanjing Tech University, Nanjing 210009, P. R. China

[5]Shenzhen Key Laboratory of Deep Underground Engineering Sciences and Green Energy, Shenzhen 518060, P. R. China

[6]WA School of Mines: Minerals, Energy and Chemical Engineering, Curtin University, Perth, Western Australia 6845, Australia

Corresponding Authors: **Heping Xie** (xiehp@szu.edu.cn); **Bin Chen** (chenbin@szu.edu.cn); **Meng Ni** (meng.ni@polyu.edu.hk)

¶: these authors contributed the equally work.

Basic characterizations

To determine the crystal structure of the BF, BF-C and re-BF powders, the room-temperature powder X-ray diffraction was performed (XRD, Bruker D8 Advance, Germany). The variation of crystal structures with temperature were characterized using the in situ high-temperature X-ray diffraction (HTXRD, Rigaku D/max 2500 V) technique; the measurements were performed on a powder diffractometer equipped with a high-temperature attachment and with the air evacuated from the sample chamber into the vacuum state, followed by replenishment of atmosphere with highly pure CO_2 repeatedly to ensure the sample chamber of the attachment is filled with CO_2. The heating rate was 10 K min^{-1}, and the temperature was held for 20 min at each temperature step. Powder X-ray diffraction patterns at both room

temperature and high temperature were collected by step scanning over the range of 2θ = 10-90° using filtered Cu-K_α radiation from a source operated at 40 kV and 40 mA with a receiving slit of approximately 0.2-0.4 mm in width and at a scan rate of 10° min^{-1}. The morphologies of composite powders and cells were examined using spherical aberration-corrected transmission electron microscopy, (STEM-HAADF, FEI, Titan Cubed Themis G201), high-resolution transmission electron microscopy (HR-TEM, JEOL JEM-2100F) and a scanning electron microscope (SEM, FEI QUANTA-2000 and SEM, Hitachi S4800) under an acceleration voltage of 20 kV. The carbon dioxide desorption curve from the processed powders was investigated using TG-MS (TG analysis was performed on a thermobalance (STA 449 F3 Jupiter, NETZSCH)), and the qualitative determination of gas components emitted (CO_2) was conducted in a mass spectrometer (QMS 403D Aëolos, NETZSCH)), as previously reported. For each measurement, 10 mg of the sample was set in an alumina crucible to be introduced into the furnace of the TG-DTA at room temperature and then heated to 1000 °C at a rate of 5°C min^{-1} under argon flow. Alumina powder was used as the reference material. Gaseous products formed by pyrolysis were identified through the use of a mass spectrometer at the sampling interval of 0.1 sec. The ionisation for MS was performed by electron impact, in which the voltage and the current for acceleration were set at 70 eV and 60 μA, respectively. Thermogravimetric analysis (TGA, model STA 449 F3, Netzsch) under synthetic air from room temperature to 1000°C. The heating and cooling rate was 10°C min^{-1}. The X-ray photoelectron spectroscopy (XPS) data were collected by a Physical Electronics PHI 5600 multi-technique system using Al monochromatic X-ray at a power of 350 W. For the Fourier transform-infrared (FT-IR) spectroscopy measurements, powders were mixed with dried KBr and then pressed into disks. The FT-IR analyses were performed on a NEXUS-670 FT-IR spectrometer (Thermo Nicolet, USA) in the frequency range of 800-2000 cm^{-1} at a resolution of 2 cm^{-1} and a scanning number of 150. The spectra were collected using the KBr contained disks in transmission mode. All TEC tests were performed using a Netzsch DIL 402C/3/G dilatometer in air with a heating rate of 5°C min^{-1}.

Thermodynamics of carbonation reaction

Thermodynamic analysis of carbonation reaction for oxides are conducted in HSC software to evalutate their reactivity to CO_2 from 400 and 800°C. The Gibbs free energy change (ΔG) is used as the indicator of thermodynamic stability of carbonates at given temperatures [S1]. Among all the listed metal oxides, the reaction between BaO and CO_2 is the most spontaneous according to the largest negative value of ΔG.

Supporting Figures

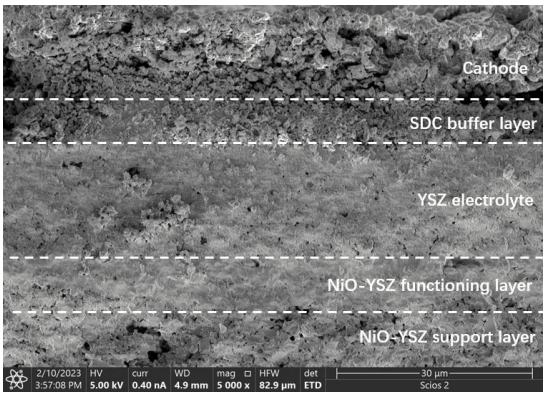

Figure S1 Cross-sectional SEM image of single cell.

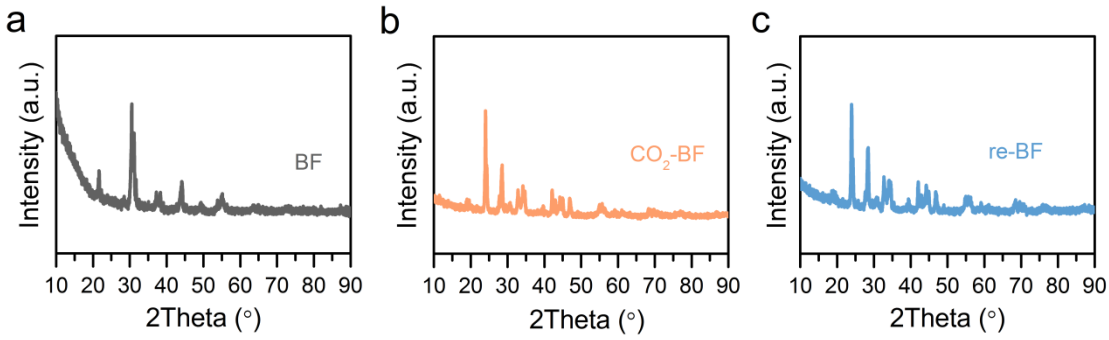

Figure S2 The XRD curves of **a)** BF, **b)** CO_2-BF and **c)** re-BF.

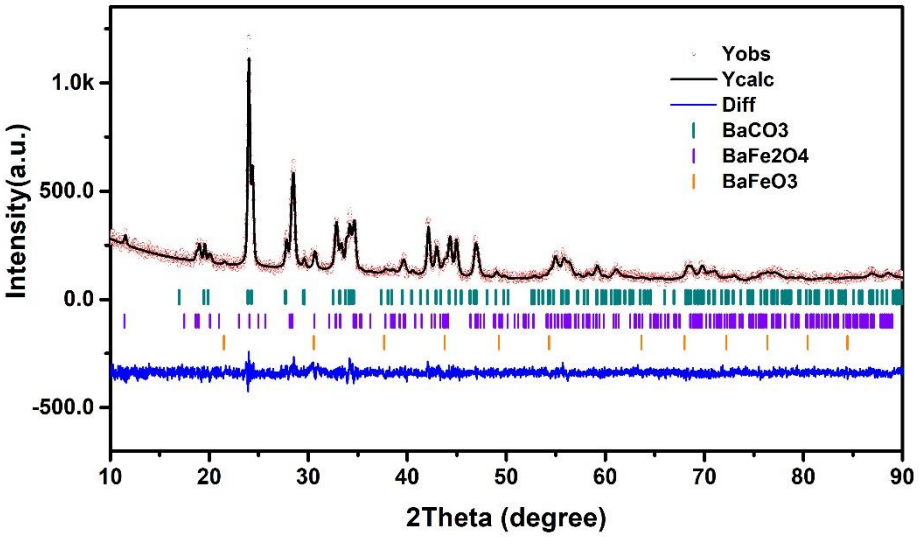

Figure S3 The XRD refinement result of CO_2-BF, consisting of three different phases: the Rhombohedral $BaFeO_3$ phase (space group: R3mR, ~4.29 wt.%, a=b=c=4.0994 Å), the Orthorhombic phase $BaFe_2O_4$ (space group: *Bb21m*, ~39.84 wt.%, a=19.1487 Å, b=5.4257 Å and c=8.5287 Å) and a phase of Orthorhombic $BaCO_3$ (space group: *Pmcn*, ~ 55.87wt.%, a=5.3325 Å, b=8.9471 Å and c=6.6185 Å)

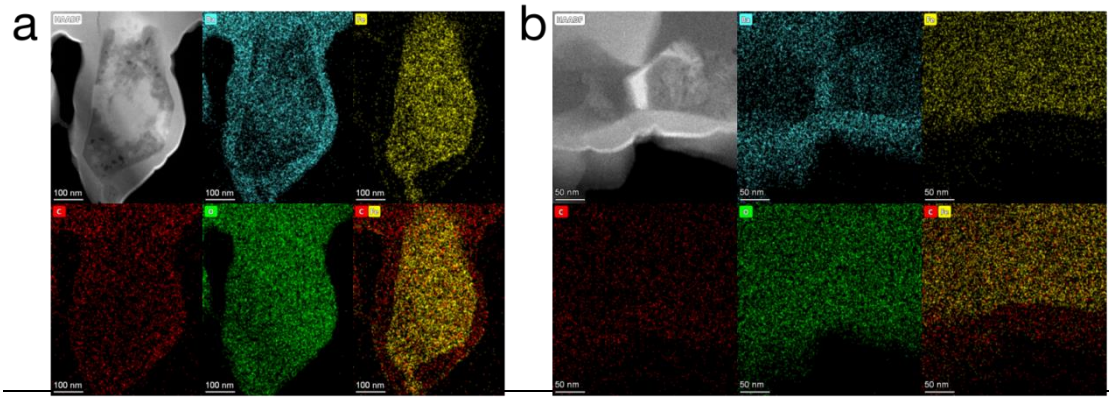

Figure S4 (a) and **(b)** STEM-EDX mapping images for re-BF at two different positions .

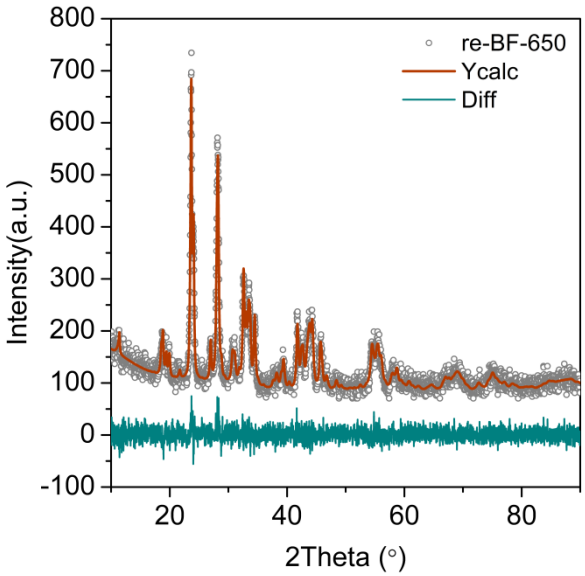

Figure S5 Refinement result of XRD profile for re-BF at 650°C. The finial re-BF consists of three different phases: the Rhombohedral $BaFeO_3$ phase (space group: R3mR, ~9.78 wt.%, a=b=c=4.0994 Å), the Orthorhombic phase $BaFe_2O_4$ (space group: *Bb21m*, ~42.15 wt.%, a=19.1487 Å, b=5.4257 Å and c=8.5287 Å) and a phase of Orthorhombic $BaCO_3$ (space group: *Pmcn*, ~ 48.07wt.%, a=5.3325 Å, b=8.9471 Å and c=6.6185 Å)

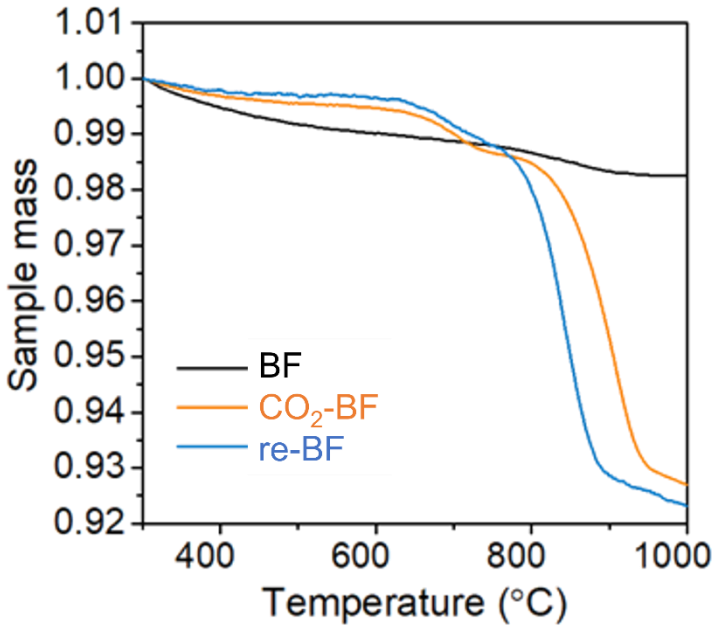

Figure S6 TGA profile of BF, CO_2-BF and re-BF cathode.

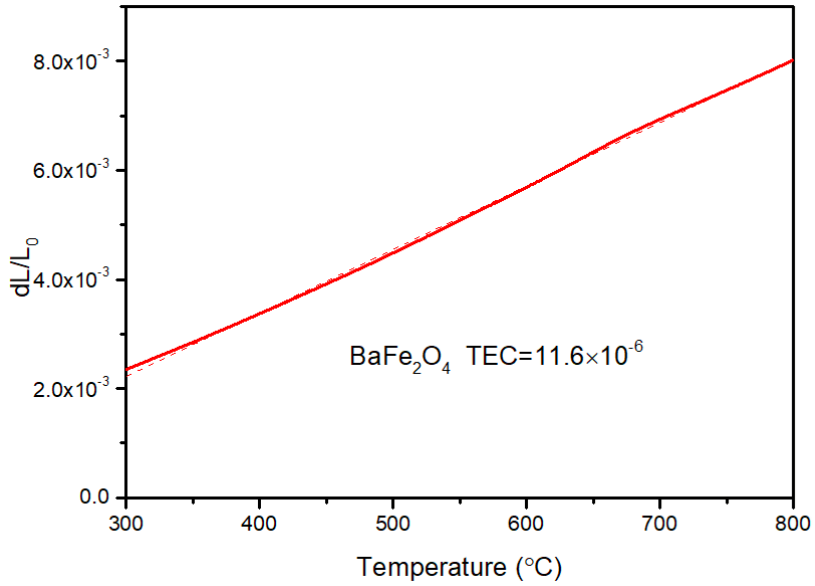

Figure S7 TEC measurement for $BaFe_2O_4$ from 300°C to 800°C.

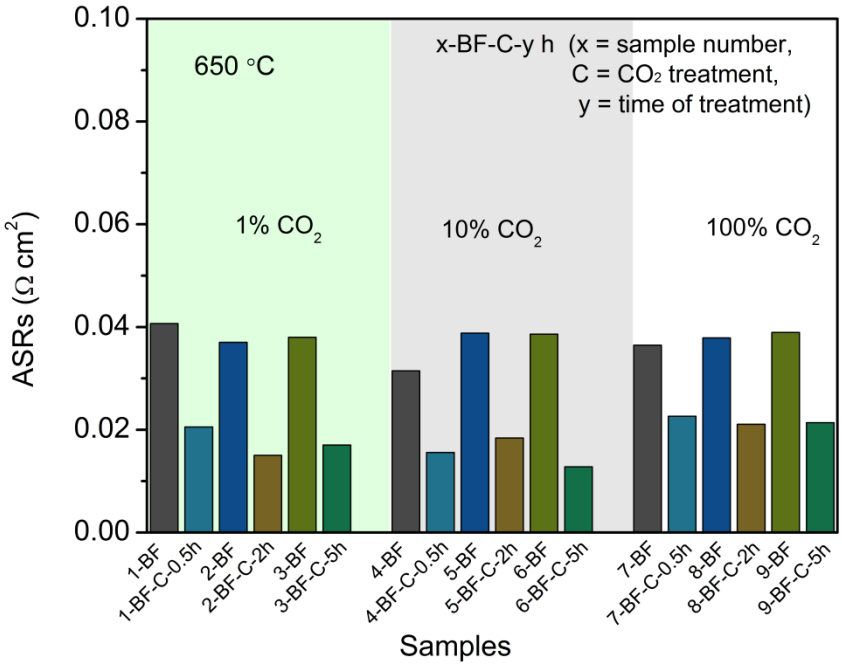

Figure S8 The ASRs of BF cathode before and after the treatment of CO_2 at different concentrations (1%, 10% and 100%) for different time (0.5 h, 2 h and 5 h), and after steady in air for 5 h at 650°C.

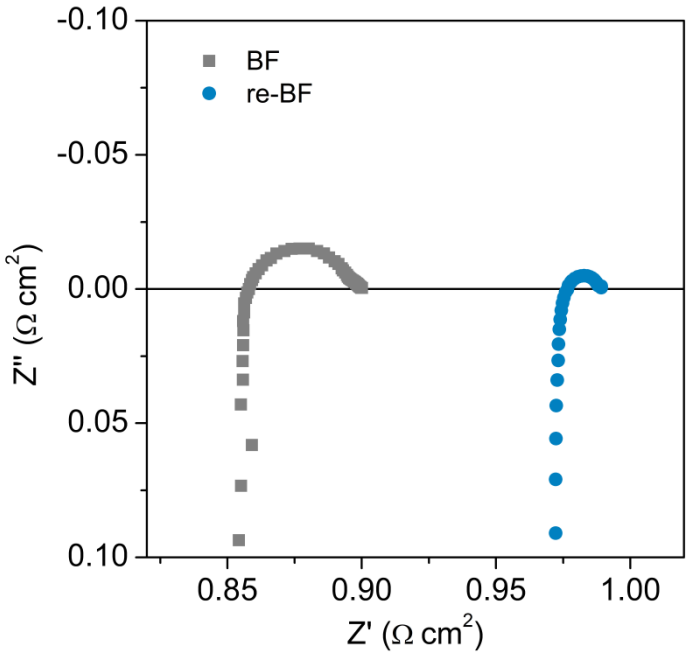

Figure S9 The EIS curves with ohmic resistance for re-BF and BF cathode at 650°C.

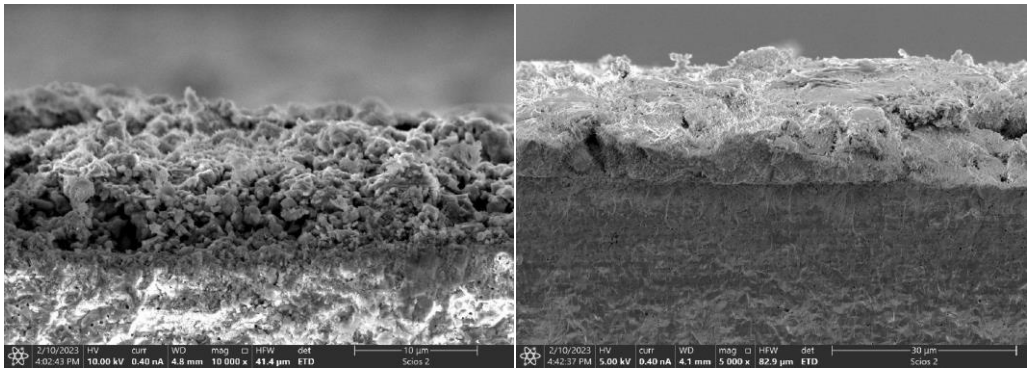

Figure S10 SEM picture of electrode cross-sections: (a) re-BF cathode; (b)$BaCO_3$ impregnated cathode.

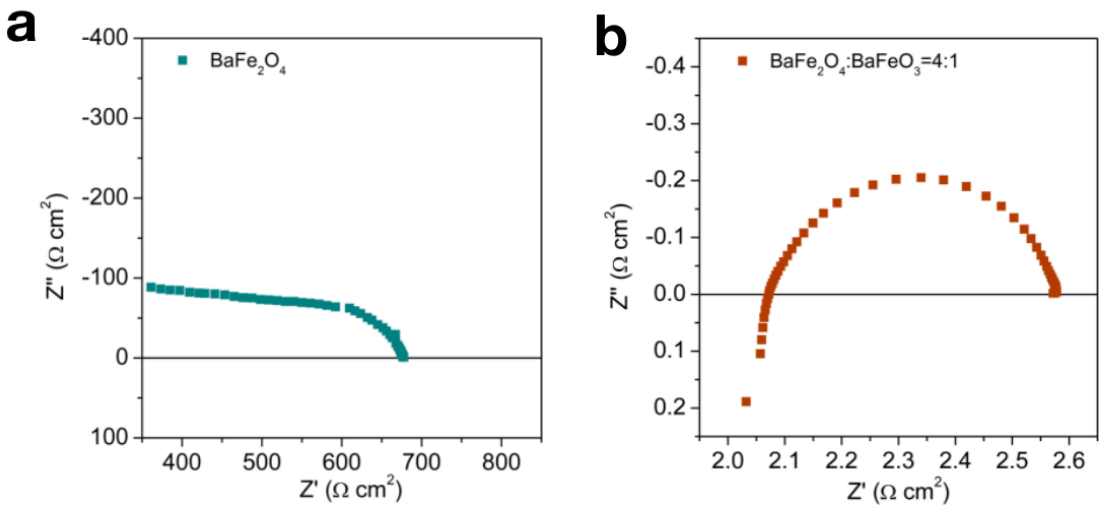

Figure S11 EIS of mixture cathode with (a) $BaFe_2O_4$ and (b) $BaFe_2O_4$:$BaFeO_3$=4:1wt at 650°C.

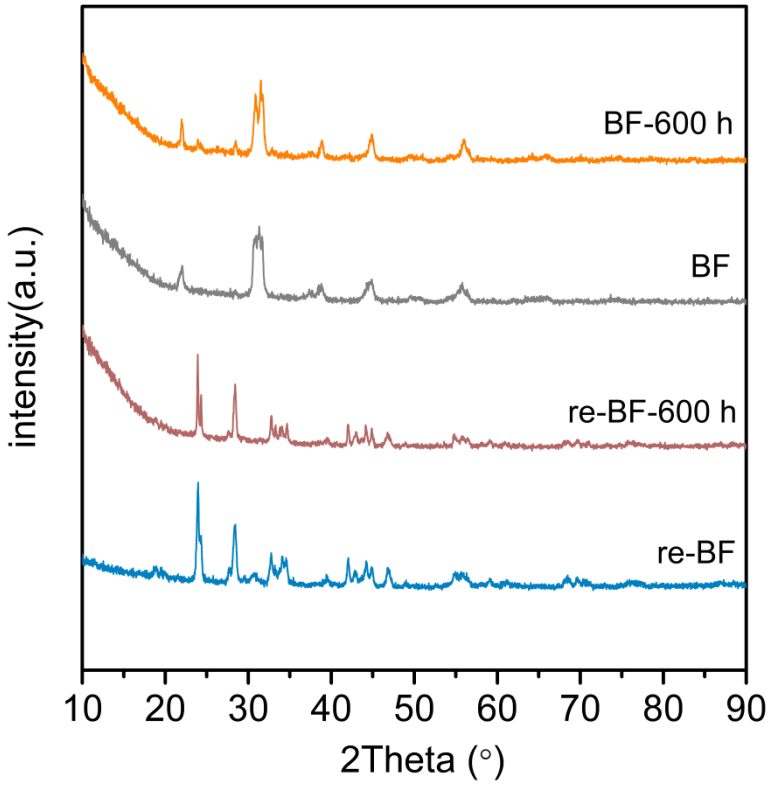

Figure S12 The XRD patterns of re-BF and BF cathodes after 600 h treatment in air at 650°C.